Constraining the subunit order of rod cyclic nucleotide-gated channels reveals a diagonal arrangement of like subunits

Yejun He, MariaLuisa Ruiz*, and Jeffrey W. Karpen†

Department of Physiology and Biophysics, University of Colorado School of Medicine, Denver, CO 80262

Edited by Denis Baylor, Stanford University School of Medicine, Stanford, CA, and approved November 19, 1999 (received for review October 5, 1999)

Retinal rod cyclic nucleotide-gated channels are composed of α and β subunits. We have explored possible subunit arrangements by expressing tandemly linked dimers of both subunits and examining their responses to three different modulating agents. Channels formed from either α-β or β-α heterodimers had functional properties similar to those formed from coexpressed α and β monomers and to native channels. These results point to an α-β-α-β arrangement. To ensure that heterodimers had not flipped around, we coexpressed α-α dimers with an excess of either β monomers or β-β dimers. Our data indicate that heteromultimers do not form efficiently in an α-α-β-β arrangement. Thus, we propose that native rod cyclic nucleotide-gated channels are arranged with like subunits diagonally opposed: α-β-α-β.

Cyclic nucleotide-gated (CNG) channels play a central role in visual transduction in retinal rod and cone photoreceptor cells (1, 2). These channels generate the electrical response to light. In photoreceptor outer segments, a light-activated enzyme cascade decreases the cytoplasmic cGMP concentration causing CNG channels to close (3, 4). This produces a membrane hyperpolarization that leads to a decreased release of glutamate onto second-order neurons. A similar CNG channel generates the electrical response to odorants in olfactory receptor neurons (5). CNG channels have been shown to be expressed in many other tissues where their functions remain to be determined (6, 7).

Retinal rod CNG channels are activated by the binding of at least three molecules of cGMP (8–12). Molecular cloning and extensive biochemical experiments have demonstrated that these channels are composed of two types of subunits: α and β (10, 13–17). Each subunit contains a single cGMP-binding site near its cytoplasmic C terminus (18, 19). Although these channels are relatively insensitive to membrane potential, the transmembrane topology of each subunit is like that of voltage-gated channel subunits, i.e., six transmembrane domains (TMs), and a pore region between TM5 and TM6 (20, 21). Like voltage-gated potassium channels (22, 23), there is evidence that retinal CNG channels function as tetramers (11, 24–26). In heterologous expression systems, α subunits can form functional channels by themselves, but their properties are distinct from native channels (13). In contrast, when β subunits are expressed on their own, no cGMP-induced currents are detected. However, when α and β subunits are coexpressed, the resulting heteromeric channels have functional properties more like those of native channels (15, 16).

Recently, the arrangement of subunits in heteromeric rod CNG channels was investigated by using Ni^{2+} as a probe (27). Ni^{2+} potentiates the action of cyclic nucleotides in CNG channels (28–30). A prior study of α-subunit homomultimers had suggested that Ni^{2+} is coordinated by α-H420 residues on adjacent subunits (24). Operating on the assumption that histidines on adjacent subunits must also coordinate Ni^{2+} in heteromeric channels, the recent study (27) concluded that Ni^{2+} is coordinated by α subunits alone in an α-α-β-β arrangement. However, neither the stoichiometry nor the arrangement of subunits was constrained.

To constrain the order of subunits in the native rod channel, we made a variety of tandem dimeric cDNA constructs of bovine rod channel α and β subunits. This approach has been used successfully in the study of potassium channels (31–34), as well as retinal and olfactory CNG channels (24–26, 35). Expressed CNG channels coded by the dimeric constructs were probed with two agents that have been used to distinguish between homomeric channels consisting of the α subunit alone and heteromeric channels formed from α and β subunits (whose properties resemble native channels): the channel blocker *l-cis*-diltiazem and the partial agonist cAMP. The results indicate that native rod channels assemble with like subunits diagonally opposed, rather than adjacent to each other. Moreover, our data suggest that the β subunit within a heteromeric channel can interact with Ni^{2+} and participate in potentiation.

Materials and Methods

Molecular Biology. Full-length cDNA clones of α (13) (gift of W. Zagotta, University of Washington, Seattle) and β (16) (gift of R. Molday, University of British Columbia, Vancouver) subunits of the bovine rod channel were subcloned into the high-expression pGEM-HE vector (33). The tandem dimer constructs were made by joining the coding sequences of two subunits together into a single ORF. To ensure that the concatenated subunits could assume the correct transmembrane topology for normal channel function, we inserted a 15-aa linker $[(gly)_7leu(gly)_7]$ between the subunits. The dimer constructs were made by using PCR and subcloning techniques. In brief, a half-linker sequence was attached to the appropriate terminus of each protomer sequence, and the stop codon of the leading protomer sequence was deleted. The sequence of each half-linker region was constructed with an *Avr*II site for joining the two protomer sequences together. The sizes of the dimeric DNA and RNA were confirmed by gel electrophoresis. Restriction enzyme mapping was performed on the dimers to confirm the subunit orientation. The linkers and the flanking sequences were sequenced to verify that there were no second-site mutations. We used the QuickChange Site-Directed Mutagenesis Kit (Stratagene) to generate single amino acid point mutations (αH420Q, βC1010A, and βH1040A). For deletion of the glutamic acid-rich protein (GARP) region of the β subunit (α-β^{GARP-}, see *Results*), a *Stu*I site was introduced into the α-β dimer at base pair position 2307 (GARP, 2288–4000). There is an existing *Stu*I site at base pair position 3981. *Stu*I digestion

This paper was submitted directly (Track II) to the PNAS office.

Abbreviations: CNG, cyclic nucleotide-gated; GARP, glutamic acid-rich protein.

*Present address: Entelos, Inc., 4040 Campbell Avenue, Suite 200, Menlo Park, CA 94025.

†To whom reprint requests should be addressed. E-mail: Jeffrey.Karpen@UCHSC.edu.

The publication costs of this article were defrayed in part by page charge payment. This article must therefore be hereby marked "*advertisement*" in accordance with 18 U.S.C. §1734 solely to indicate this fact.

deleted the fragment in between (2307–3981). For all constructs, mRNAs were transcribed from cDNAs *in vitro* with the mMESSAGE mMACHINE T7 Kit (Ambion, Austin, TX) and microinjected into *Xenopus* oocytes. Each oocyte was injected with 50 nl of total mRNA at a concentration of 0.5–10 ng/nl. For heteromultimers, we typically used a 1:2.5 molar ratio of α:β subunit mRNA (unless otherwise indicated). Higher proportions of β subunit mRNA did not measurably change the heteromeric channel properties (Fig. 3). After injection, the oocytes were incubated at room temperature overnight, and at 18°C thereafter. Electrophysiological recordings were performed 2–14 days after injection.

Electrophysiology. Patch-clamp recordings of channel activity were made from excised membrane macropatches in the inside-out configuration by using an Axopatch 1D amplifier (Axon Instruments, Foster City, CA). Recordings were at room temperature. Electrodes had resistances of 0.7–1.5 MΩ. Currents evoked by a 200-ms step to −50 mV from a holding potential of 0 mV were low-pass filtered at 1 kHz and sampled at 5 kHz. Some experiments were done at +50 mV for comparison, and this did not alter any of the conclusions. At low concentrations of cGMP, currents were measured in the steady-state; at high concentrations, currents were measured 2 ms after switching the voltage to minimize the effects of ion accumulation and depletion (36). Large currents (>5 nA) were corrected for the voltage drop across the pipette series resistance. Solutions were applied to the macropatches by an RSC 100 rapid solution changer (Molecular Kinetics, Pullman, WA). The extracellular and control intracellular solutions contained (in mM): 130 NaCl, 2 Hepes (pH 7.6), 0.02 EDTA, and 1 EGTA. When 10 μM Ni^{2+} was added, EDTA and EGTA were not included. In some experiments, 500 μM niflumic acid was added to the extracellular solution to reduce background Cl^- channel activity, which did not affect the cGMP-induced currents or the response to Ni^{2+}. Cyclic GMP-activated currents were determined as the difference between currents measured in the presence and the absence of cGMP. The fraction of maximal current, I/I_{max}, was the current at a given concentration of cGMP divided by the maximal current at saturating cGMP. All cGMP dose-response relations were fit with the Hill equation: $I/I_{max} = (\text{cGMP})^n/[(\text{cGMP})^n + K_{1/2}{}^n]$, where n is the Hill coefficient, and $K_{1/2}$ is the concentration of cGMP that gives a half-maximal current. Data were expressed as mean ± standard error. cGMP and cAMP were from Sigma, and nickel chloride hexahydrate (purity > 99.9999%) was from Aldrich.

Results

Heteromeric Channels Formed from α-β or β-α Dimers Are Functionally Similar to Native Channels. Because *l-cis*-diltiazem blocks native rod channels and expressed heteromeric channels with much higher affinity than homomeric channels (15, 16, 37), we used it to probe the functional integrity of homomeric and heteromeric channels formed from tandem dimers. Fig. 1*A* shows currents through CNG channels formed from α-α (*Left*) and α-β (*Right*) dimers, in response to saturating cGMP and different concentrations of *l-cis*-diltiazem. For α-α dimers, 20 μM *l-cis*-diltiazem did not effectively block the current, whereas the same concentration blocked about 85% of the current from α-β dimers. Fig. 1*B* shows the concentration dependence of *l-cis*-diltiazem block of currents through homomeric and heteromeric channels formed from either monomers or dimers. In agreement with earlier reports, *l-cis*-diltiazem blocked heteromeric channels more effectively than homomeric channels. The concentration of *l-cis*-diltiazem that caused half-maximal inhibition, K_I, was about fifty times lower for heteromultimers than for homomultimers. The results were nearly identical for α-α dimers vs. α monomers, and α-β dimers vs. coinjected α and β monomers, suggesting that

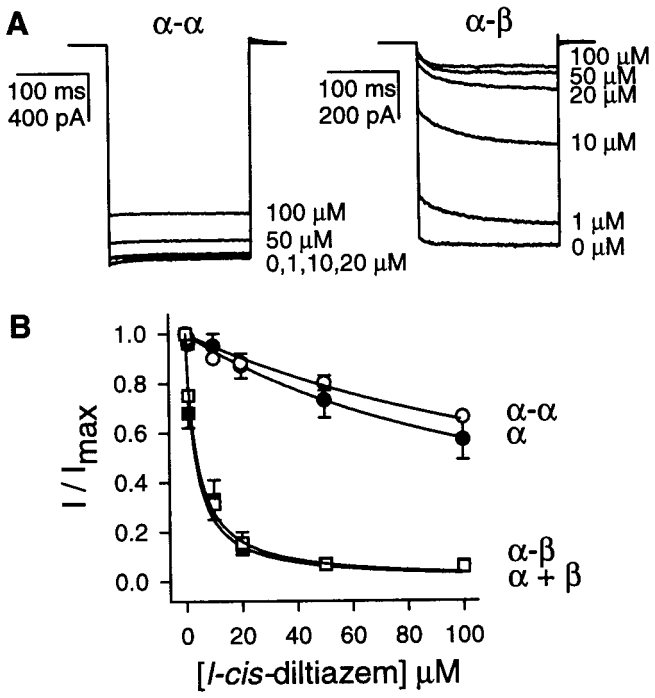

Fig. 1. *l-cis*-diltiazem blocks channels formed from α-β heterodimers more effectively than those from α-α homodimers. (*A*) Current traces elicited by saturating cGMP (1 mM) and different concentrations of *l-cis*-diltiazem in patches expressing α-α (*Left*) and α-β (*Right*) channels. Currents were evoked by −50 mV pulses from a holding potential of 0 mV. (*B*) *l-cis*-diltiazem sensitivities of homomeric and heteromeric channels formed from both monomers and dimers. The response to 1 mM cGMP in the presence of *l-cis*-diltiazem divided by the response in the absence of *l-cis*-diltiazem (I/I_{max}) is plotted against *l-cis*-diltiazem concentration. The smooth curves are fits to the data with the equation: $I/I_{max} = K_I/([l\text{-}cis\text{-diltiazem}] + K_I)$, where K_I is the concentration of *l-cis*-diltiazem that causes half-maximal inhibition. α monomers, K_I = 135 μM (n = 4); α-α dimers, K_I = 185 μM (n = 4); α + β monomers (■), K_I = 3.3 μM (n = 5); α-β dimers (□), K_I = 3.8 μM (n = 4).

both subunits of the dimers participated normally in channel function. Furthermore, 10 μM *l-cis*-diltiazem blocked currents through channels formed from β-α dimers to a very similar degree as channels formed from α-β dimers. The results with the two heterodimers suggest that channels with unlike subunits adjacent and like subunits diagonally opposed behave like native channels, at least with respect to block by *l-cis*-diltiazem.

As a further test that heterodimers mimicked the properties of expressed heteromultimers and native channels, we measured the response to saturating cAMP. cAMP is a partial agonist for CNG channels. It is a stronger agonist for native channels (38, 39) and expressed heteromeric channels (27) than for homomeric channels formed from α subunits alone (30). When dimers were tested for cAMP efficacy at −50 mV, a saturating concentration (8 mM) activated about 0.7% of the maximal current elicited by saturating cGMP from homodimers and about 6% from heterodimers. These results were indistinguishable from those obtained with α monomers and coinjected α and β monomers under the same conditions. They are also consistent with previous results on expressed and native channels, accounting for differences in membrane potential. These results suggest again that heterodimers reconstituted native channel properties.

The β subunit has an unusual bipartite structure (16): the cytoplasmic N-terminal region includes the sequence of a GARP, two isoforms of which exist as separate proteins in photoreceptors (40, 41), whereas the rest of the protein is similar

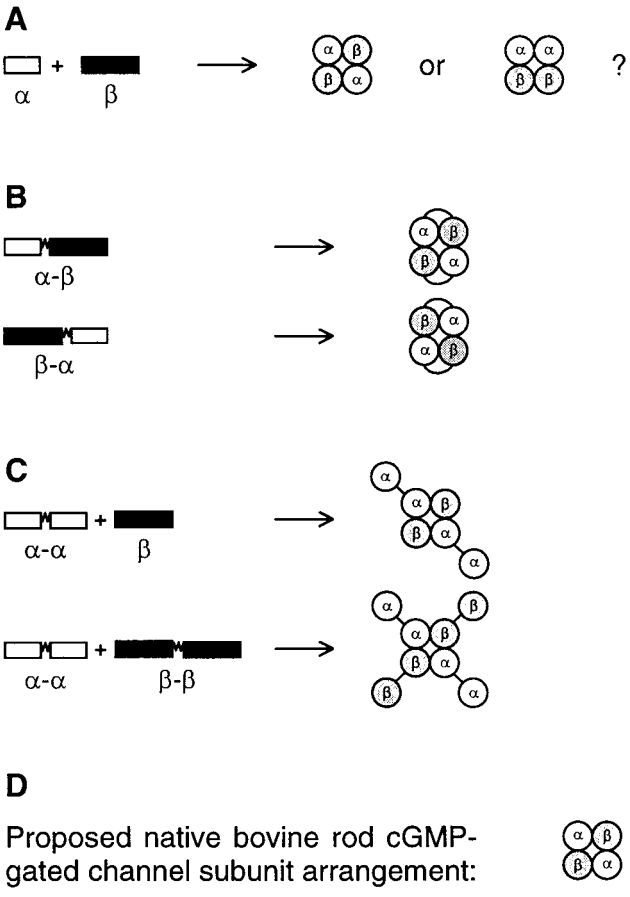

Fig. 2. Possible subunit arrangements. (*A*) The two arrangements from coexpression of α and β monomers assume that heteromeric channels are tetramers with a 2:2 subunit stoichiometry. (*B*) The most likely heteromeric channel arrangements from α-β and β-α heterodimers. (*C*) Probable functional heteromeric channel arrangements, formed inefficiently from coexpressed α-α dimers with either β monomers or β-β dimers. (*D*) Proposed subunit arrangement of native bovine rod CNG channels.

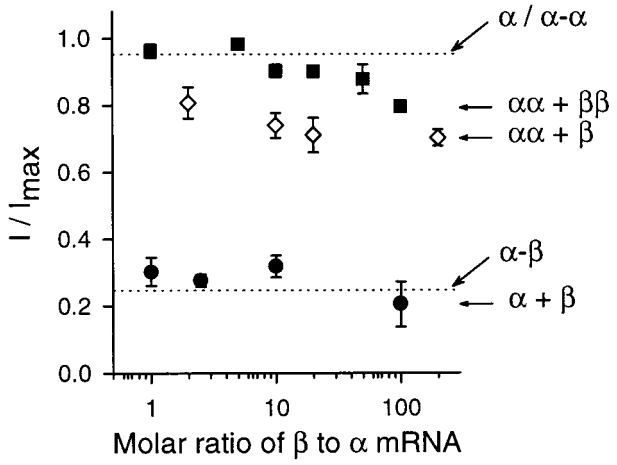

Fig. 3. *l-cis*-diltiazem sensitivities of different channel constructs. The response to 1 mM cGMP in the presence of 10 μM *l-cis*-diltiazem divided by the response in the absence of *l-cis*-diltiazem (I/I_{max}) is plotted against the ratio of injected β (or β-β) to α (or α-α) mRNAs. For all conditions $n = 4$ to 24, except a 1:20 ratio of α-α + β-β ($n = 1$). The upper dotted line indicates the average fractional current measured from α monomers and α-α dimers (0.95 ± 0.008, $n = 24$), whereas the lower dotted line is the fractional current measured from α-β dimers (0.25 ± 0.018, $n = 24$). The fractional current of α-α + β-β with a 1:10 ratio was significantly different from that of α-α + β with a 1:10 ratio ($P < 0.01$). At a 1:20 ratio, there was no overlap between the fractional currents measured from α-α + β ($n = 5$) and α-α + β-β ($n = 1$). The fractional current of α-α + β-β or α-α + β at all ratios was significantly different from α/α-α ($P < 0.01$), except α-α + β-β with 1:1 and 1:5 ratios.

to the α subunit. The β-GARP region has been shown not to affect the gross electrophysiological properties of the expressed channel (16). We were concerned that the extra length of the GARP region at the N terminus (571 aa) might confer too much slack between the α and β subunits in α-β dimers and undermine the constraint on subunit order. To test for this, we deleted most of the β-GARP region of the α-β dimers (see *Materials and Methods*), to make the distance between subunits comparable to that of the β-α dimer. As expected, dose-response relations for cGMP were not altered in the GARP deleted α-β dimers (α-$\beta^{\mathrm{GARP}-}$). *l-cis*-diltiazem block and cAMP activation were also unchanged (data not shown). Thus, we conclude that the β-GARP region does not significantly affect heterodimeric channel assembly.

α-α-β-β Is an Unfavorable Configuration in Heteromeric Rod CNG Channels. Tetrameric channels with two α and two β subunits could assemble in two possible configurations: like subunits diagonally opposed or adjacent (Fig. 2*A*). Earlier work on potassium channels and CNG channels (24, 25, 31–34) suggested that heterodimers like α-β usually assemble in a "head-to-tail" fashion, such that the resulting channels have like subunits diagonally across from each other (Fig. 2*B*). Our findings that channels formed from heterodimers have several properties in common with native channels suggest that rod CNG channels assemble with like subunits diagonally opposed. However, these data do not rule out the possibility that heteromeric channels could assemble with like subunits adjacent to each other. There are three possible scenarios. First, α-α-β-β could be an alternative channel arrangement. Second, it could be the preferred channel arrangement, if the subunit protomers of one heterodimer are able to switch positions with each protomer still maintaining a correct orientation for pore formation. Third, it could also be the preferred channel arrangement if the protomers of each dimer can separate enough to assemble diagonally across from each other. There is evidence from previous studies that the latter two scenarios are possible (42, 43). However, these artifacts may have occurred because much longer intersubunit linkers were employed (24–64 residues vs. 15 residues in this study).

We investigated whether the α-α-β-β configuration is favorable by coexpressing α-α dimers with either β monomers or β-β dimers. Whether dimers flip around or not would result in the same α-α-β-β arrangement. We used *l-cis*-diltiazem sensitivity as a measure of the fraction of functional heteromultimers formed with different combinations of monomers and dimers. The fractional current in 10 μM *l-cis*-diltiazem is plotted as a function of the molar ratio of β to α mRNA in Fig. 3. The upper dotted line is the average fractional current in the presence of *l-cis*-diltiazem for homomultimers formed from α monomers and α-α dimers. The lower dotted line is the fractional current in the presence of *l-cis*-diltiazem for α-β dimers. When α and β subunit monomers were coexpressed, at all different ratios tested, the fractional remaining current was not statistically different from that observed in α-β dimers (P ranging from 0.13 to 0.39), suggesting the majority of functional channels formed were heteromeric. Their maximal cAMP responses also supported this (data not shown). Even at a 1:1 molar ratio of β to α subunits, most of the channels formed were heteromeric, based on their *l-cis*-diltiazem sensitivity. This suggests that the favorability of

forming heteromeric channels is greater than the favorability of forming homomeric channels. If there were no preference for subunit arrangement, then at a 1:1 molar ratio of β-β to α-α dimers, we would expect that mostly heteromultimers should form. However, the fractional remaining current in the presence of *l-cis*-diltiazem was not statistically different ($P = 0.69$) from that observed in α-subunit homomultimers, suggesting that most channels were homomeric. The same result was obtained when the molar ratio of β-β to α-α dimers was increased to 5:1. Even at a 100:1 molar ratio, the fractional remaining current was still much closer to that observed in homomultimers, suggesting the majority of functional channels were homomultimers. We then coexpressed α-α dimers with β monomers. This served as an important control for the coexpression of α-α dimers with β-β dimers, since both α-α dimers and β monomers were known to be functional and to incorporate efficiently into channels. Even at a 200:1 molar ratio of β monomers to α-α dimers, most of the functional channels formed were apparently homomeric. As further evidence, the cAMP response of channels formed in all the above coexpression experiments was close to 0.7% activation, i.e., the response expected if channels were homomeric. Thus, there was little detectable heteromeric channel formation when we tried to force the channels to have like subunits adjacent to each other (α-α-β-β). We conclude that this arrangement is very unfavorable for expressed heteromeric channel assembly.

There are four possible explanations for the small amount of *l-cis*-diltiazem block observed when α-α dimers were mixed with either β monomers or β-β dimers. First, α-α-β-β channels could form easily but be blocked with low affinity by *l-cis*-diltiazem. This is unlikely because channels formed with a β-β to α-α ratio of 100:1 were significantly different from those formed with a ratio of 1:1 ($P < 0.01$). Second, they could form with very low efficiency. However, in this scenario it is difficult to explain why β-β dimers would incorporate less easily than β monomers (in fact, we would have anticipated the opposite result). Third, the protomers of α-α and β-β dimers could assemble diagonally across from each other (43). Fourth, channels could form with the leading subunits of the dimers assembling around a central pore, while the trailing subunits are left hanging off the perimeter of the channel (35, 42, 44, 45), resulting in channels with like subunits diagonally opposed (Fig. 2*C*). (It should be noted that the incorporation of trailing subunits without leading subunits has never been reported.) We favor the fourth explanation because incorporation of the β subunit was concentration-dependent, and β monomers inserted more easily than β-β dimers (which requires exclusion of two additional trailing subunits). However, it is important to note here that the degree of *l-cis*-diltiazem block was very low compared with that observed in normal heteromeric channels.

Thus, all the evidence points to the most favorable arrangement of subunits being α-β-α-β. (*i*) Coexpression of α monomers with β monomers resulted in mostly heteromeric channels. (*ii*) α-β and β-α dimers had several functional properties closely resembling those of native channels: cGMP dose-response relations, *l-cis*-diltiazem sensitivities, maximal cAMP responses, and magnitudes of Ni^{2+} potentiation. (*iii*) Coexpression of α-α dimers with an excess of either β monomers or β-β dimers did not efficiently form heteromeric channels. We propose native bovine retinal rod CNG channels have like subunits arranged diagonally across from each other (Fig. 2*D*).

Residues in Both α and β Subunits Coordinate Ni^{2+} in Native Rod CNG Channels. In expressed homomeric channels composed of bovine rod α subunits, there is evidence that the mechanism of Ni^{2+} potentiation involves intersubunit coordination of Ni^{2+} by H420 residues on adjacent subunits, which stabilizes the open conformation of the channel (24, 30). We observed strong Ni^{2+} potentiation of heteromeric channels with like subunits diagonally opposed to each other (Fig. 4). In fact, heteromultimers and homomultimers were potentiated by Ni^{2+} to a similar degree ($P = 0.12$). H420 is the only residue in the α subunit that has been reported to coordinate Ni^{2+} in homomeric channels. The corresponding residue in the β subunit is a nonnucleophilic asparagine, which is unable to coordinate transition metal ions. Subunit order was constrained in our heterodimers, such that H420 residues on the two α subunits were not adjacent to each other (see Fig. 2*B*). Thus, if no residues in the β subunit could interact with Ni^{2+}, we would expect little or no Ni^{2+} potentiation. However, our observations that Ni^{2+} potentiated heteromultimers and homomultimers to a similar degree suggest that some residue(s) in the β subunit interacts with Ni^{2+}.

To test this idea, we mutated the H420 residues in the α subunits. In agreement with a previous report (30), when all four α-H420 residues in the channel were mutated to glutamines (αH420Q), Ni^{2+} caused no significant change in $K_{1/2}$ (Fig. 4). However, when we expressed a heterodimer with the H420 residue in the α subunit mutated to glutamine (αH420Q-β),

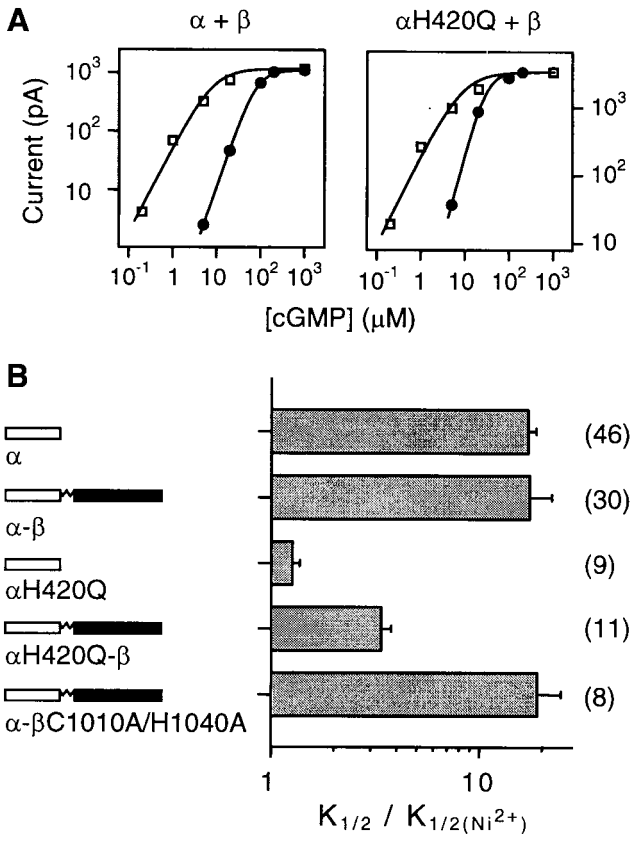

Fig. 4. Residues in the β subunit also interact with Ni^{2+}. (*A*) cGMP dose-response relations for heteromeric channels formed from $\alpha + \beta$ monomers (*Left*) and αH420Q + β monomers (*Right*). Data are shown before (●) and after (□) potentiation by 10 μM Ni^{2+}. Smooth curves are fits to the Hill equation (see *Materials and Methods*). $\alpha + \beta$: pre-Ni^{2+}, $n = 2.2$, $K_{1/2} = 83$ μM; post-Ni^{2+}, $n = 1.5$, $K_{1/2} = 8.6$ μM. αH420Q + β: pre-Ni^{2+}, $n = 2.4$, $K_{1/2} = 31$ μM; post-Ni^{2+}, $n = 1.3$, $K_{1/2} = 8.7$ μM. The corresponding dimer constructs behaved very similarly. (*B*) Sensitivity of different channel constructs to Ni^{2+}. The abscissa is the factor change in $K_{1/2}$ in the presence of Ni^{2+}. Number of experiments indicated in parentheses. The average fold changes in $K_{1/2}$ are: α (including α-α), 17 ± 1.6; α-β (including $\alpha + \beta$), 16 ± 3.2; αH420Q, 1.3 ± 0.1; αH420Q-β (including αH420Q + β), 3.4 ± 0.4; α-βC1010A/H1040A (including $\alpha + \beta$C1010A/H1040A), 19 ± 5.6. The apparent affinity changes between α and αH420Q, between αH420Q-β and α-β, and between αH420Q and αH420Q-β were different ($P < 0.01$).

potentiation still occurred, although to a lesser degree than that observed in wild-type α-β channels. The apparent affinity for cGMP increased by an average of 3.4-fold in the presence of Ni^{2+} (Fig. 4). Coexpression of αH420Q monomers with wild-type β subunit monomers yielded the same results. Incorporation of β subunit was confirmed by *l-cis*-diltiazem. This Ni^{2+} potentiation was intermediate between that observed in αH420Q mutants and wild-type α-β channels ($P < 0.01$). It was also observed with different lots of high-purity $NiCl_2$. Since the two histidine residues on the α subunits required for Ni^{2+} potentiation were mutated, the result suggests that the two β subunits interact with Ni^{2+} to cause potentiation. A smaller degree of potentiation was expected, because only two subunits were presumably interacting with Ni^{2+}. Moreover, like subunits were diagonally across from each other, suggesting that residues on adjacent subunits may not be required for Ni^{2+} potentiation of heteromultimers.

Which residue(s) in the β subunit coordinate Ni^{2+}? Although the residue corresponding to α-H420 is N1019 in the β subunit, there is a histidine residue in the vicinity at position 1040. Besides histidine, cysteine can also coordinate transition metal ions, and there is a cysteine residue at position 1010. We thought that these residues might interact with Ni^{2+}, so we mutated both of them to alanines. Surprisingly, heteromultimers with the double mutation in the β subunit (wild-type α subunit with βC1010A/H1040A) were still strongly potentiated by Ni^{2+}. The average Ni^{2+}-induced change in the apparent affinity for cGMP was 19.0-fold (Fig. 4), similar to that observed in wild-type homomultimers and heteromultimers. To eliminate coordination of Ni^{2+} by the two wild-type α subunits, we made a triple mutant, in which α-H420 was mutated to glutamine and the β subunit had the two mutations C1010A and H1040A. This triple mutant dimer (αH420Q-βC1010A/H1040A) was potentiated to a lesser degree by Ni^{2+} (6-fold increase in apparent affinity, two patches), comparable to the potentiation observed in α-β dimers with the H420Q mutation (αH420Q-β). These data indicate that residue(s) other than C1010 or H1040 in the β subunit can interact with Ni^{2+}.

Discussion

In this study, we have made tandem dimers of the α and β subunits of the bovine rod CNG channel to investigate the preferred subunit arrangement. We found expressed channels formed from either α-β or β-α dimers, with like subunits diagonally opposed, had several functional properties in common with native channels, including *l-cis*-diltiazem sensitivity, cAMP activation, and Ni^{2+} potentiation. Coexpression of α-α dimers with an excess of either β-β dimers or β monomers yielded mostly homomultimers, suggesting that it is unfavorable for functional heteromultimers to be formed with like subunits adjacent to each other. The only scenario in which the data in this paper would support an α-α-β-β arrangement is if each of the four dimer constructs (α-β, β-α, α-α, and β-β) *forces* the protomers to assemble diagonally. This is precisely the opposite of what dimers are intended to do, and seems extremely unlikely in principle. Could α-β and β-α heterodimers favor any other channel configuration? Artifacts in which the leading subunit incorporates but the trailing subunit does not (35, 42, 44, 45) could possibly yield α-α-α-β (from α-β dimers) and β-β-β-α (from β-α dimers) arrangements (assuming at least one α subunit is required for channel expression, and at least one β subunit is required for high-affinity *l-cis*-diltiazem block). But the very similar responses to *l-cis*-diltiazem and cAMP between α-β and β-α dimers make these configurations unlikely. Therefore, the simplest explanation for our results is that retinal rod CNG channels have a 2:2 stoichiometry of α and β subunits with like subunits diagonally across from each other: α-β-α-β (Fig. 2*D*).

A recent study by Shammat and Gordon (27) concluded that rod CNG channels assemble in the α-α-β-β configuration. There was no attempt to constrain the subunit stoichiometry or arrangement in this work. Instead, the conclusion rests entirely on a previous study of α-subunit homomultimers (24) in which evidence was presented by using tandem dimers that Ni^{2+} potentiates channel activity when H420 residues are present on adjacent subunits, but not when they are present only on diagonally opposed subunits. In the recent work (27), the large reduction in Ni^{2+} potentiation of heteromeric channels observed when α-H420 was replaced with glutamine, and the enhancement observed when histidines were placed in the equivalent position of the primary sequence of the β subunit, were interpreted to mean that like subunits must be adjacent in heteromeric channels. However, there is not enough known about the three-dimensional structure of these channels to conclude that proximity relationships in α-subunit homomultimers must apply to heteromultimers containing α and β subunits. The β subunit is larger than the α subunit; the two subunits are only about 30% homologous over the domains in common; assembly of heteromeric channels is favored over assembly of homomeric channels (Fig. 3; see also ref. 27); and heteromeric channels have a number of properties distinct from those of homomultimers. All of these observations suggest that the structures and subunit relationships in homomultimers may not apply to heteromultimers. An important difference between our results and those of Shammat and Gordon is that we find β subunits can apparently interact with Ni^{2+} and contribute to potentiation (Fig. 4). We observed similar potentiation of homomultimers and heteromultimers, and significant potentiation (3.4-fold decrease in $K_{1/2}$, 11 patches) of expressed heterodimers with the critical α subunit histidine replaced with glutamine (αH420Q-β). In channels formed by coexpressing αH420Q and β, Shammat and Gordon observed a shift in the dose-response relation and an enhancement in the effect of cAMP by Ni^{2+} on individual patches. However, these effects were deemed not statistically significant when results from different numbers of patches in each condition were averaged (four patches in the presence of Ni^{2+}, and six in the absence), where $K_{1/2}$ and the maximal cAMP response exhibited large intrinsic patch-to-patch variabilities. Instead, we have used the standard deviations of the *ratios* of $K_{1/2}$ in the absence and presence of Ni^{2+} *on the same patch* to test for significance (Fig. 4). With β subunits apparently able to coordinate Ni^{2+} and participate in potentiation, the necessity for adjacent α subunits is no longer compelling. We suggest that residues on adjacent α and β subunits might coordinate Ni^{2+}, or alternatively, residues on nonadjacent subunits, a different mechanism than homomultimers.

For all subunit combinations tested, we usually (but not always) observed a shallower dose-response relation (lower Hill coefficient) in the presence of Ni^{2+} than in the absence. This was found previously in a study of native salamander rod channels (29). In contrast, Gordon and Zagotta (24, 30) did not observe any significant Ni^{2+}-induced shallowing for expressed α-subunit homomultimers. We duplicated their recording conditions and still observed shallower dose-response relations in the presence of Ni^{2+}. We also compared Ni^{2+} potentiation at +50 and −50 mV, but no systematic difference was observed. The channel Gordon and Zagotta studied had an alanine to valine substitution at position 483, which is close to the cGMP-binding domain. This reportedly caused a small decrease in the channels' apparent affinity for cGMP. In the recent study by Shammat and Gordon (27), shallower dose-response relations in the presence of Ni^{2+} were observed for some constructs and not others. Although we have not discovered why the shallowing in the presence of Ni^{2+} occurs, this did not affect our conclusions.

The degree of Ni^{2+} potentiation observed in native amphibian channels (29) was smaller than that in expressed homomeric (24,

30) and heteromeric channels (ref. 27 and the present study). We suspect these are species differences, since the two subunits used for heterologous expression were cloned from bovine retina. In this vein, it is interesting to note that the maximal cAMP-induced current in native amphibian channels was 25% of the maximal cGMP-induced current (38), vs. only 10% for native bovine channels (39) and expressed heteromultimers.

The native olfactory CNG channel now appears to be composed of three different subunits, two of which are similar to the rod α subunit, and one of which is similar to the rod β subunit (46–49). The stoichiometry and arrangement of the three subunits has not been investigated. A study of the assembly of the two α-like subunits using tandem dimers (35) concluded that they assemble with like subunits adjacent to each other, but it is not clear whether this has any bearing on the assembly of the more disparate α and β subunits.

CNG channels that are similar or identical to those present in rods, cones, and olfactory receptors have been found in a variety of nonsensory tissues, where their roles are largely unknown. Knowing the stoichiometry and arrangement of subunits is crucial for understanding the function of a channel in its cellular setting. It also provides a foundation for examining the structural basis of channel gating and permeation.

We thank Drs. R. L. Brown, A. Ghatpande, and T. Rich for comments on the manuscript, and S. Gordon (University of Washington) for sending us a sample of the $NiCl_2$ used in her experiments for comparison. *l-cis*-diltiazem was the gift of Dr. K.-W. Yau (Johns Hopkins University, Baltimore). This work was supported by National Institutes of Health Grants EY09275 (to J.W.K.) and EY06713 (individual National Research Service Award to ML.R.).

1. Fesenko, E. E., Kolesnikov, S. S. & Lyubarsky, A. L. (1985) *Nature (London)* **313,** 310–313.
2. Yau, K.-W. & Baylor, D. A. (1989) *Annu. Rev. Neurosci.* **12,** 289–327.
3. Pugh, E. N., Jr., & Lamb, T. D. (1993) *Biochim. Biophys. Acta* **1141,** 111–149.
4. Molday, R. S. (1998) *Invest. Ophthalmol. Visual Sci.* **39,** 2491–2513.
5. Nakamura, T. & Gold, G. H. (1987) *Nature (London)* **325,** 442–444.
6. Finn, J. T., Grunwald, M. E. & Yau, K.-W. (1996) *Annu. Rev. Physiol.* **58,** 395–426.
7. Wei, J.-Y., Roy, D. S., Leconte, L. & Barnstable, C. J. (1998) *Prog. Neurobiol.* **56,** 37–64.
8. Haynes, L. W., Kay, A. R. & Yau, K.-W. (1986) *Nature (London)* **321,** 66–70.
9. Zimmerman, A. L. & Baylor, D. A. (1986) *Nature (London)* **321,** 70–72.
10. Cook, N. J., Hanke, W. & Kaupp, U. B. (1987) *Proc. Natl. Acad. Sci. USA* **84,** 585–589.
11. Ruiz, M. L. & Karpen, J. W. (1997) *Nature (London)* **389,** 389–392.
12. Ruiz, M. L., Brown, R. L., He, Y., Haley, T. L. & Karpen, J. W. (1999) *Biochemistry* **38,** 10642–10648.
13. Kaupp, U. B., Niidome, T., Tanabe, T., Terada, S., Bönigk, W., Stühmer, W., Cook, N. J., Kangawa, K., Matsuo, H. & Hirose, T. (1989) *Nature (London)* **342,** 762–766.
14. Cook, N. J., Molday, L. L., Reid, D., Kaupp, U. B. & Molday, R. S. (1989) *J. Biol. Chem.* **264,** 6996–6999.
15. Chen, T.-Y., Peng, Y.-W., Dhallan, R. S., Ahamed, B., Reed, R. R. & Yau, K.-W. (1993) *Nature (London)* **362,** 764–767.
16. Körschen, H. G., Illing, M., Seifert, R., Sesti, F., Williams, A., Gotzes, S., Colville, C., Müller, F., Dosé, A., Godde, M., *et al.* (1995) *Neuron* **15,** 627–636.
17. Colville, C. A. & Molday, R. S. (1996) *J. Biol. Chem.* **271,** 32968–32974.
18. Brown, R. L., Gerber, W. V. & Karpen, J. W. (1993) *Proc. Natl. Acad. Sci. USA* **90,** 5369–5373.
19. Brown, R. L., Gramling, R., Bert, R. J. & Karpen, J. W. (1995) *Biochemistry* **34,** 8365–8370.
20. Heginbotham, L., Abramson, T. & MacKinnon, R. (1992) *Science* **258,** 1152–1155.
21. Henn, D. K., Baumann, A. & Kaupp, U. B. (1995) *Proc. Natl. Acad. Sci. USA* **92,** 7425–7429.
22. MacKinnon, R. (1991) *Nature (London)* **350,** 232–235.
23. Doyle, D. A., Morais, C. J., Pfuetzner, R. A., Kuo, A., Gulbis, J. M., Cohen, S. L., Chait, B. T. & MacKinnon, R. (1998) *Science* **280,** 69–77.
24. Gordon, S. E. & Zagotta, W. N. (1995) *Proc. Natl. Acad. Sci. USA* **92,** 10222–10226.
25. Liu, D. T., Tibbs, G. R. & Siegelbaum, S. A. (1996) *Neuron* **16,** 983–990.
26. Varnum, M. D. & Zagotta, W. N. (1996) *Biophys. J.* **70,** 2667–2679.
27. Shammat, I. M. & Gordon, S. E. (1999) *Neuron* **23,** 809–819.
28. Ildefonse, M. & Bennett, N. (1991) *J. Membr. Biol.* **123,** 133–147.
29. Karpen, J. W., Brown, R. L., Stryer, L. & Baylor, D. A. (1993) *J. Gen. Physiol.* **101,** 1–25.
30. Gordon, S. E. & Zagotta, W. N. (1995) *Neuron* **14,** 177–183.
31. Isacoff, E. Y., Jan, Y. N. & Jan, L. Y. (1990) *Nature (London)* **345,** 530–534.
32. Heginbotham, L. & MacKinnon, R. (1992) *Neuron* **8,** 483–491.
33. Liman, E. R., Tytgat, J. & Hess, P. (1992) *Neuron* **9,** 861–871.
34. Pascual, J. M., Shieh, C.-C., Kirsch, G. E. & Brown, A. M. (1995) *Neuron* **14,** 1055–1063.
35. Shapiro, M. S. & Zagotta, W. N. (1998) *Proc. Natl. Acad. Sci. USA* **95,** 14546–14551.
36. Zimmerman, A. L., Karpen, J. W. & Baylor, D. A. (1988) *Biophys. J.* **54,** 351–355.
37. Stern, J. H., Kaupp, U. B. & MacLeish, P. R. (1986) *Proc. Natl. Acad. Sci. USA* **83,** 1163–1167.
38. Furman, R. E. & Tanaka, J. C. (1989) *Biochemistry* **28,** 2785–2788.
39. Gavazzo, P., Picco, C., Maxia, L. & Menini, A. (1996) in *Properties of Native and Cloned Cyclic Nucleotide Gated Channels from Bovine*, eds. Torre, V. & Conti, F. (Plenum, New York), pp. 75–83.
40. Sugimoto, Y., Yatsunami, K., Tsujimoto, M., Khorana, H. G. & Ichikawa, A. (1991) *Proc. Natl. Acad. Sci. USA* **88,** 3116–3119.
41. Körschen, H. G., Beyermann, M., Müller, F., Heck, M., Vantler, M., Koch, K.-W., Kellner, R., Wolfrum, U., Bode, C., Hofmann, K. P. & Kaupp, U. B. (1999) *Nature (London)* **400,** 761–766.
42. Zheng, J. & Sigworth, F. J. (1998) *J. Gen. Physiol.* **112,** 457–474.
43. Morrill, J. A. & MacKinnon, R. (1999) *J. Gen. Physiol.* **114,** 71–83.
44. McCormack, K., Lin, L., Iverson, L. E., Tanouye, M. A. & Sigworth, F. J. (1992) *Biophys. J.* **63,** 1406–1411.
45. Hurst, R. S., North, R. A. & Adelman, J. P. (1995) *Recept. Channels* **3,** 263–272.
46. Dhallan, R. S., Yau, K.-W., Schrader, K. A. & Reed, R. R. (1990) *Nature (London)* **347,** 184–187.
47. Liman, E. R. & Buck, L. B. (1994) *Neuron* **13,** 611–621.
48. Sautter, A., Zong, X., Hofmann, F. & Biel, M. (1998) *Proc. Natl. Acad. Sci. USA* **95,** 4696–4701.
49. Bönigk, W., Bradley, J., Müller, F., Sesti, F., Boekhoff, I., Ronnett, G. V., Kaupp, U. B. & Frings, S. (1999) *J. Neurosci.* **19,** 5332–5347.